Linking dispersal connectivity to population structure and management boundaries for saithe, *Pollachius virens* (Linnaeus, 1758) in the northeast Atlantic

Mari S. Myksvoll[1*], Jennifer Devine[2], María Quintela[1], Audrey J. Geffen[3], Richard D. M. Nash[1,4], Anne Sandvik[1], François Besnier[1], Atal Saha[5], Geir Dahle[1], Eeva Jansson[1], Kjell Nedreaas[1], Torild Johansen[6]

[1]Institute of Marine Research, P.O. 1870, Nordnes, N-5817 Bergen, Norway

[2]National Institute of Water and Atmospheric Research (NIWA), 217 Akersten Street, Port Nelson, Nelson 7010, New Zealand

[3]Department of Biological Sciences, University of Bergen, PO Box 7800, 5020 Bergen, Norway

[4]Present address: Centre for Environment, Fisheries and Aquaculture Science (Cefas), Pakefield Road, Lowestoft, Suffolk, NR33 0HT, UK

[5]Department of Zoology, Division of Population Genetics, Stockholm University, 10691 Stockholm, Sweden

[6]Institute of Marine Research, Framsenteret, 9296 Tromsø, Norway

[*]Corresponding author: mari.myksvoll@hi.no

Keywords: egg buoyancy, egg stage duration, genetic population structure, individual-based modelling, SNP markers, ROMS

Running page head: Saithe population connectivity

ABSTRACT

Population connectivity is an increasingly important focal area for the understanding of how marine fish populations respond to anthropogenic pressures like climate change and fisheries management. Our model species, saithe, is chosen because genetic analyses have documented a mismatch between the assessed stocks and the biological populations. We combine laboratory experiments of saithe egg buoyancy and temperature modulated development time, genetic field data, and high-resolution oceanographic models to disentangle the mechanisms causing isolation and mixing between the management units and the biological populations. Saithe egg buoyancy and development data were included in an individual-based model to simulate transport from all known spawning grounds in the northeast Atlantic. The results show that the interannual variability in transport of early life stages is strongly influenced by wider climate systems (e.g. NAO, North Atlantic Oscillation). One genetic sample (Rockall) showed genetic differences from the other samples which was supported by the model showing low mixing with other populations and strong local retention. Strong retention of early life stages around Iceland could indicate an isolated population; however, this is counteracted by active migration of adults westward from the Norwegian coast and no genetic differentiation is found. Overall, the dispersal modeling supports the genetic analysis, showing a large and well connected Central Northeast Atlantic population distributed across several management units. This mismatch can potentially increase the risk for overexploitation of saithe.

1. INTRODUCTION

Population connectivity is an increasingly important focal area for understanding the functioning of the marine environment, particularly as research has demonstrated that marine fish populations rarely have panmictic population structure, but fall along a continuum, with the majority having numerous district populations (Kerr et al. (2017) and references therein). Understanding of connectivity can help determine how species respond and recover from anthropogenic or climatic changes (Secor et al. 2009), and is necessary for devising effective fisheries management strategies (Fogarty & Botsford 2007). The degree of connectivity can be determined by inspecting whether populations are genetically separated or if mixing of demographic traits occurs at some point in their life history.

Genetic connectivity is commonly measured as the extent of allele sharing between populations and is defined as the degree to which gene flow affects evolutionary processes within the population (Lowe & Allendorf 2010). The distribution of genetic variation within and among populations is determined by the interaction between natural selection and neutral evolutionary processes. The way environmental variation shapes neutral and adaptive genetic variation in natural populations is a key issue in evolutionary biology that has implications for the sustainable management of the populations. Many marine fish species display a weak genetic population structure due to the combined effect of large population size coupled with high gene flow (Ward et al. 1994). As a consequence, most of genetic markers may be uninformative about demographic processes, which has fuelled the search for loci carrying signatures of locally divergent selection that might serve as powerful markers to assess spatially explicit genetic structure as well as to outline stocks for fisheries management (Russello et al. 2012). High genetic connectivity does not necessarily mean that

only a single population unit exists because relatively occasional exchange per generation can result in the appearance of genetic homogeneity (Hawkins et al. 2016).

The contribution of dispersal to population connectivity in marine populations largely occurs through the exchange of planktonic larvae, although migration of adults and mixing at the spawning grounds may also occur (Cowen et al. 2000, Hawkins et al. 2016). Planktonic larvae dispersal is largely influenced by physical processes (e.g., currents, fronts, eddies, tides, boundary layers; Werner et al. (1997)), the time scale of egg and larval development, including swimming and behavioral capabilities, and the location and timing of spawning (Cowen et al. 2000, Pineda et al. 2007). Hydrodynamical models with individual-based models (IBM) are useful tools to study dispersal connectivity between early life stages (Myksvoll et al. 2014). In the northern part of the northeast Atlantic, these tools have been mainly applied to Northeast Arctic cod (*Gadus morhua*) (Vikebø et al. 2007), Norwegian coastal cod (Myksvoll et al. 2014), and Norwegian Spring Spawning herring (*Clupea harengus*) (Vikebø et al. 2012). More recently the spatiotemporal modeling has expanded to also include Northeast Arctic haddock (*Melanogrammus aeglefinus*) (Castaño-Primo et al. 2014), polar cod (*Boreogadus saida*) (Huserbråten et al. 2019), glass eel (*Anguilla anguilla*) (Cresci et al. 2021), and salmon lice (*Lepeophtheirus salmonis)* (Sandvik et al. 2020).

The main objective of this work is to quantify the connectivity in a common marine fish species in the North Atlantic, using dispersal models and genetic tools. Our model species is saithe (*Pollachius virens*). Genetic differentiation has been observed within the saithe stock, where populations were genetically distinct in the western Atlantic Ocean from those in the eastern Atlantic, and at least three distinct populations were identified in the eastern Atlantic (Saha

et al. 2015), but the question remains if finer population structure is genetically discernable. Demographic connectivity for early life stages is investigated using a biophysical model coupled to a hydrodynamic archive, which is then compared with the results of the genetic analyses. Temperature-dependent development rates and egg buoyancy experiments provide relevant data on egg duration and potential vertical location in the water columns for the biophysical models of egg and larval drift, allowing the combination of laboratory experiments, genetic field data, and high-resolution oceanographic models will help to define biological populations and disentangle the mechanisms causing isolation and mixing between saithe populations in the Northeast Atlantic.

2. MATERIAL AND METHODS

2.1 Study species

Saithe is a gadoid fish widely distributed across the North Atlantic. The species in the northeast Atlantic has traditionally been divided into four management units (stocks) irrespective of biological or genetic population structure (Reiss et al. 2009). For the purpose of clarification, we interpret *Management Units* as geographical areas (using the ICES (International Council for the Exploration of the Sea) subarea and division designations), *Stocks* as assessed areas and/or groups of fish, and *Populations* as genetically identified groups of interbreeding individuals that are at least moderately reproductively isolated from others. Currently, ICES assess and provide a single catch advice for four saithe stocks (Figure 1): Icelandic (ICES division 5a), Faroes (ICES division 5b), Northeast Arctic (including the Norwegian coast and the Barents Sea, ICES subareas 1 and 2), and North Sea (including Rockall/West of Scotland and the Skagerrak; subareas 4 and 6 and division 3a). The management units, or areas, with their

associated Total Allowable Catches (see EU-TOR (2020)) correspond with the stock assessment designation for the Faroes and Iceland, but the Northeast Arctic stock has two management units (Norwegian waters of subareas 1 and 2 and International waters of subareas 1 and 2) and the North Sea stock has four management units (division 3a and subarea 4 plus EU waters of 2a; Norwegian waters south of 62° N; subarea 6 plus EU and international waters of division 5b, including subareas 12 and 14; and subareas 7, 8, 9 and 10 plus Union waters of CECAF (Fishery Committee for the Eastern Central Atlantic) 34.1.1). The Icelandic and Northeast Arctic stocks are considered to be harvested sustainably (ICES 2019, 2020a), whereas the stocks from the North Sea and Faroes are currently fished above levels that allow sustainable harvest albeit spawning stock biomass is still deemed to be above the precautionary level (ICES 2020b, c).

Saha et al. (2015) identified four genetic clusters (Rockall, Central Northeast Atlantic, Barents Sea, Canada) across the species' range in the North Atlantic. Despite being genetically distinct, the Rockall cluster is assessed as part of the North Sea stock, and the Barents Sea cluster is included with the Norwegian coastal fish as the Northeast Arctic stock. The large Central Northeast Atlantic cluster, which included the Norwegian coastal and North Sea saithe, is currently managed and harvested in four separate management units.

The Institute of Marine Research (Bergen, Norway) performed a comprehensive monitoring program of fish eggs and larvae from 1986 to 1992 (HELP – Havforskningsinstituttets egg- og larveprogram); and most of our current knowledge on the distribution of saithe eggs and larvae was gained during this period. Using these data, Bjørke and Sætre (1994) hypothesized

that the northern North Sea supplies recruits of saithe along the central and northern Norwegian coast, and contributions from Faroes and west of Scotland could be expected in specific years, depending on oceanographic conditions. In addition, Bjørke and Sætre (1994) suggested that the North Sea, west of Scotland and the Faroes supplied the recruitment to the Northeast Arctic stock south of 66° N, while recruitment north of 66° N was driven by spawning along the Norwegian coast. The movement of larval and juvenile saithe from the North Sea to the Norwegian coast has been suggested since the early 1900s (Damas 1909). Saithe are abundant along the Norwegian coast at all life history stages (Mehl et al. 2011), but there is some debate about the connectivity between offshore spawning and the inshore nursery areas for juveniles. Northeast Arctic cod and saithe spawn in almost the same areas (off the west coast of Norway) yet the juvenile nursery areas are widely separated (Mehl et al. 2011, Yaragina et al. 2011), suggesting very different drift trajectories for the early life history stages. Juvenile saithe (25-50 mm in length) are generally considered to settle inshore in very shallow water (Bertelsen 1942, Lie 1961, Mironov 1961). A similar behavior and size at settlement is also seen in the western Atlantic (Steele 1963, Clay et al. 1989). Inshore spawning of saithe has previously been considered negligible, and may still be, but has been documented by genetic analyses of eggs and larvae in Norwegian fjords since 2010 (Torild Johansen, IMR, Norway, *pers. com.*). Mature saithe may be attracted by unconsumed food and faeces emanating from salmon aquaculture farms, and then spawn in the fjords instead of returning offshore to the traditional spawning grounds (Dempster et al. 2009, Otterå & Skilbrei 2014).

2.2 Study area

The geographical distribution of saithe in the northeast Atlantic is shown in Figure 1. We focused on the assumed spawning populations, which included the spawning areas at Rockall, Faroes, Iceland, northern North Sea, and the Norwegian coast. The total area was divided into boxes for calculating connectivity between regions (see small map in Figure 1), named Rockall (ROC), Faroes (FAR), Iceland (ICE), North Sea West (NSW), North Sea East (NSE), Møre (MOR), Halten (HAL), and Barents Sea (BAR). The Barents Sea box includes everything north of Halten. The box West of Britain (WOB) is included specifically to evaluate transport from Rockall outside of the main study area.

2.3 Genetic analysis

Saithe population structure, defining biological populations, was determined from genetic analysis of tissue samples collected from all stocks in the northeast Atlantic and from the Gulf of Maine (USA) between 2010 and 2019 (Figure 1 and Table S2). Compared to our previous study (Saha et al. 2015), where the number of fish in each sample was limited to 48, in this study, the number of fish per sample was increased, and the number of samples from the Northeast Arctic stock was not only increased to nine but the sampling time was focused in winter, close to the spawning season. The sample from Faroes and Rockall are the same as in Saha et al. (2015) but with a slightly larger number of individuals, 74 and 50, respectively. The samples were composed of immature, maturing, and spawning fish. Samples collected from only spawning fish were difficult to obtain because the spawning of saithe is protracted, the peak in spawning differs between stocks (Olsen et al. 2010, Mehl et al. 2011, Homrum et al. 2012), and surveys or the fisheries may not occur in the area during peak spawning.

DNA was extracted from gill filaments using the E-Z 96 Tissue omega DNA Kit (Omega Bio-Teck, Inc.) following the manufacturer's protocol. DNA was quantified using a broad range double-strand kit on a Qubit fluorometer (Life Technologies Corp.), and quality was checked by agarose gel electrophoresis. A suite of specially-devoted SNPs was developed from new pool sequencing (Johansen et al. in prep) covering a wider distribution area compared to Saha et al. 2015, and 111 loci distributed in four multiplexes were selected and genotyped on 1202 individual fish. After trimming loci showing bad clustering as well as individuals with >30% missing markers, the final data set consisted of 1087 saithe genotyped at 77 SNP loci. SNP amplification and genotype calling was performed using the Sequenom MassARRAY iPLEX Platform, as described by (Gabriel et al. 2009). PCR conditions are available in the Supplementary Material.

Conformance with linkage phase equilibrium (LD) and Hardy-Weinberg proportions (HWE) were examined for all markers and samples using GENEPOP 7 (Rousset 2008). The observed (H_o) and unbiased expected heterozygosity (uH_e) as well as the inbreeding coefficient (F_{IS}) per sample were computed with GenAlEx v6.1 (Peakall & Smouse 2006). Loci influenced by selection can reveal genetic differentiation and hence improve the definition of conservation units and outline locally adapted populations (Nielsen et al. 2009, Funk et al. 2012, Nielsen et al. 2012). Two analytic approaches, BayeScan (Foll & Gaggiotti 2008) and LOSITAN (Antao et al. 2008), were used to detect loci deviating from neutral expectations which therefore reflect either eventual selective responses or linkage disequilibrium with genes under divergent selection (Lewontin & Krakauer 1973). In BayeScan, sample size was set to 10 000 and the thinning interval to 50. Loci with a posterior probability over 0.99, corresponding to a Bayes Factor >2 (*i.e.* “decisive selection” (Foll & Gaggiotti 2006)), were retained as outliers. In

LOSITAN, a neutral distribution of F_{ST} with 1 000 000 iterations was simulated, with forced mean F_{ST} at a significance level of 0.05 under an infinite allele model. Overall and pairwise genetic differentiation was assessed with F_{ST} (Weir & Cockerham 1984) computed with ARLEQUIN v.3.5.1.2 (Excoffier et al. 2005). The relationship among geographically explicit samples was also examined via the Discriminant Analysis of Principal Components (Jombart et al. 2010) implemented in *adegenet* (Jombart 2008). A number of principal components ranging from 10 to 60 was tested to determine the optimal number of PCs necessary to avoid overfitting of the data and creating artificially large separation between groups (Jombart & Collins 2015, Miller et al. 2020). The trade-off between power of discrimination and overfitting was measured using the a-score, which is the difference between the proportion of successful reassignment of the analysis (observed discrimination) and values obtained using random groups (random discrimination); in other words, the proportion of successful reassignment corrected for the number of retained PCs. Genetic structure was also investigated via Principal Coordinates Analysis (PCoA) implemented in GenAlEx v6.1 (Peakall & Smouse 2006) using the pairwise F_{ST} between samples as a distance matrix. To examine the demographic relationships between geographically explicit samples, the pairwise genetic distance, measured as $F_{ST}/(1-F_{ST})$, was correlated with the corresponding geographic distance through a Mantel test using GenAlEx v6.1 (Peakall & Smouse 2006).

2.4 Experimental determination of egg stage duration and egg specific gravity

Realistic drift modelling relies on information about the buoyancy of eggs and the duration of the egg stage over a range of temperatures. The temperature dependence of egg development, from soon after fertilization to hatching, was determined using a temperature gradient block experiment (Geffen & Nash 2012). Egg specific gravity was determined for eggs

233 from the same spawning batches in temperature-controlled density columns (Jung et al.
234 2012). Laboratory experiments were conducted in 2017 and 2018 with eggs collected from a
235 captive broodstock consisting of six females and three males, established in 2013 at the
236 Institute of Marine Research Austevoll research facility from wild-caught North Sea saithe.
237 These fish first spawned in 2014 (Skjæraasen et al. 2017), and continued to spawn annually.
238 Egg collectors were fitted to the holding tanks and checked daily during the spawning period.
239 Water temperature in the spawning tanks was approximately 4°C. Eggs were spawned at night
240 and collected within 12 hours of fertilization.
241
242 **2.4.1 Duration of egg development from fertilization to hatch**
243 Egg development experiments started on 11th March 2017 and 24th February 2018 with eggs
244 at stage IA (Geffen et al. 2006), corresponding to stage 7/8 of Fridgeirsson (1978) description
245 of saithe stages of development. The eggs were transferred at 4^{o}C from the broodstock facility
246 to a temperature-controlled room at the Department of Biological Sciences, University of
247 Bergen. The eggs were divided into four batches and slowly acclimated, over a period of 4-6h
248 to 4^{o}C, 6^{o}C, 8^{o}C, and 10^{o}C by the gradual addition of warmer water. Once the eggs reached
249 the target temperature, they were placed into 2.5 L incubation chambers situated in the
250 temperature gradient block. Egg density was approximately 500 L^{-1} to allow for regular
251 sampling.
252
253 The temperature gradient block is a self-contained insulated unit with a heating element at
254 one end and a cooling unit at the other end creating a controlled temperature gradient over
255 the length of a large acrylic box (Geffen & Nash 2012). The incubation chambers were placed
256 along the gradient to give nominal temperatures of 4^{o}C, 6^{o}C, 8^{o}C, and 10°C. These chambers

were covered to reduce evaporation and cross-contamination. Water circulation and aeration in the chambers was driven by an air lift, creating a gentle current to drive continuous movement of water and eggs from the bottom of the chamber to the water surface. The water in each chamber was refreshed daily by exchanging at least 50% of the volume with new water adjusted to the correct temperature. Water temperatures were monitored continuously with temperature probes in each chamber linked to an overall monitoring system. At least 10 eggs were sampled daily from each incubation chamber from day 1 (1 DAF, days after fertilization) until hatching was complete. These eggs were staged and photographed for later measurement of egg size and for a record of development. In addition to these experiments, four batches of eggs were held in incubation tanks at the IMR experimental research facility at Austevoll (from spawning events on the 20th, 29th March and 3rd April 2019). Here, temperature was monitored daily and the time to start, 50% and 100% of the eggs hatching was recorded. These data provide additional information on a limited number of temperatures (6.0^{o}C to 6.8^{o}C) but a greater range of 'batches' of eggs. The temperature dependence of time from fertilization (DAF) to 50% of the eggs hatching was fit using linear models (lm) on log transformed average recorded temperatures and DAF.

2.4.2 Egg buoyancy estimation

Egg buoyancy was estimated from measurements of specific density, determined using density- gradient columns, as described by Jung et al. (2012). Three individual columns were mounted in a waterbath with a clear viewing window, placed in a temperature-controlled room, where air temperature varied between 7-9°C. A salinity gradient was prepared in each column by introducing a mixture of gradually increasing salinity through a thin tube at the bottom of the column. Four spherical glass floats (density calibrated at 23°C, and accurate to

281 + 0.0002 g cm^{-3}) were placed in each column to calibrate the salinity gradient against column
282 depth. The calibration density was corrected for the column water temperature (T), according
283 to:

284 Calibration float density at T = Density + (23 – T) x 0.000028.

285 The calibration floats were left to settle for 1h before the first measurements, and 24h before
286 introducing eggs. Completed density gradients ranged between 1.015 and 1.031 (salinity
287 19.24 to 40.01) in 2017 and 1.018 to 1.033 (salinity 21.65 to 42.83) in 2018.

288

289 Egg density measurements in 2017 were conducted with eggs transferred from three of the
290 temperature block incubating chambers on day 5 after fertilization. This allowed us to assess
291 differences in density with development stage in parallel, although we missed data from the
292 earliest stages. All eggs were acclimated to the density-gradient column temperatures
293 gradually over a period of 4-6h, before 60-80 eggs were added to each column. The eggs were
294 introduced slowly at the top of each column with a large-bore pipette to minimize disruption
295 of the gradient. The eggs originating from different incubation temperatures were not mixed,
296 but were placed in separate columns. Eggs from 4° C were at development stage II (Geffen et
297 al. 2006), equivalent to stage 13/14 (Fridgeirsson 1978) at the time of transfer to the column.
298 Eggs from 6°C were at development stage II/III, equivalent to stage 16/18; and eggs from 8°C
299 were at development stage IV, equivalent to stage 21. The eggs remained in the buoyancy
300 chamber through hatching and into the yolk-sac larval stage. Specific gravity readings were
301 taken twice daily, with a minimum of one hour before the first reading to allow the eggs to
302 reach equilibrium in the column.

303

In 2018 eggs were transferred directly to the density columns from the broodstock facility, in order to obtain density estimates from the early egg development stages. Approximately 80 eggs, at stage 1A / 7/8, were transferred into each column. Specific gravity readings were taken daily, with the first reading after the eggs reached equilibrium in the column.

Moribund eggs, which were clearly discernible because they turned opaque and sank downwards, were not included in the measurements. Despite using a cooling, recirculation system and a climate-controlled room, water temperature in the buoyancy chamber varied between 7°C and 9°C throughout development; average temperature experienced by the eggs within the columns was estimated to be 8°C.

2.5 Individual-based model for saithe

The hydrography and ocean current fields were extracted from a ROMS (Regional Ocean Modeling System, www.myroms.org) model archive at 4km x 4km horizontal resolution and 32 sigma layers in the vertical (Lien et al. 2014, Sandvik et al. 2016). Based on daily temperature, salinity and current fields, the transport of saithe eggs and larvae was calculated using an open source Lagrangian particle tracking model (https://github.com/bjornaa/ladim). The advection of particles was calculated using a 4^{th}-order Runge-Kutta scheme, solving the Lagrangian equation of motion with a timestep dt=1800s. The simulations were performed for the years 1985-2017. The hydrodynamic model archive was produced in a continuous simulation (Lien et al. 2014) while the particle tracking model was run separately for each year covering the larval drift period.

Northeast Arctic saithe spawn in winter with a peak at the end of February (Olsen et al. 2010, Mehl et al. 2011), while Faroes saithe spawning typically peaks prior to mid-March (Homrum et al. 2012). In this model approach we have chosen continuous spawning, i.e. daily releases of particles, through February and March for all spawning areas, 1773 particles per day meaning 104 607 particles in total every year. Bjørke and Sætre (1994) indicate that there might be differences in spawning time, however there are no data on this to include in the model. The eggs are released at 200 m depth at all spawning areas (see small map in Figure 1), and due to positive buoyancy, they rise quickly towards the surface. The eggs are 1.0-1.2 mm in diameter (Olsen et al. 2010, Mehl et al. 2011). We used the experimentally determined relationships (section 2.4) to set the time to hatching (60 degree-days) and an average buoyancy of 32.48 ± 1.14 (see section 3.2 and Table 1). Höffle et al. (2013) showed that saithe larvae have a diurnal migration between 60 m depth during day and 30 m during night. We tested several parameterizations of vertical diurnal behavior triggered by light availability in their specific depth; however, the dispersal pattern was not very sensitive to differences as long as the larvae remained below 20 m depth. In the final model set-up, we kept the larvae between 30 m and 60 m depth. The larvae were tracked from spawning time (February/March) until mid-May, being close to the time of settling for saithe, however the settling process itself was not included in the model setup. We compared the larval distributions estimated by the IBMs under contrasting conditions of climate forcing, identified by years with positive or negative North Atlantic Oscillation (NAO) index. Monthly NAO index data were downloaded from NOAA (https://www.cpc.ncep.noaa.gov/products/precip/CWlink/pna/nao.shtml), and a winter NAO index was calculated as a mean of January, February and March.

3. RESULTS

3.1 Genetic populations

Thirteen loci displaying overall deficit of heterozygotes were removed, thus leaving 1087 individuals genotyped at 64 markers that are compiled in Table S1. Tests for LD conducted on these 64 loci proved significant in 1018 out 32 256 cases (3.15%) and dropped to 13 (0.04%) after Bonferroni correction. Departures from HWE were registered in 60 out of the 1024 loci by sample tests (5.85%), which dropped to 5 (0.49%) after Bonferroni correction. Both H_o and uH_e took similar values in all the samples (Table S2). Outlier detection methods did not meet consensus: LOSITAN reported two markers under positive selection (NS_1604_7031 and Rand_394_51901) whereas BayeScan did not detect any loci deviating from neutrality. Major allele frequency per candidate loci under selection did not seem to follow any geographic pattern (Table S3).

AMOVA revealed low but significant overall differentiation (F_{ST}=0.001, P=0.025) with 99.88% of the variation hosted within populations. Pairwise F_{ST} ranged between 0.000 and 0.018 (Table 2). All of the sampled areas, except Vesterålen, Lofoten_2017 and Storegga-Møre were significantly different from the Gulf of Maine. Saithe samples from Rockall were only significantly different from Vesterålen, Lofoten_2017 and Storegga-Møre, albeit with lower values of F_{ST}. Most of the remaining comparisons did not significantly differ from zero. In addition, the spawning sample from Lofoten_2019 was significantly different from the North Sea, Faroe and Lofoten_2017. Information about sex distribution was not available for the Gulf of Maine fish, which were therefore excluded from further analyses. Overall genetic differentiation was not significant for either sex (female F_{ST}=0.001, P=0.126; male F_{ST}=0.000,

374 P=1). Pairwise F_{ST} for males revealed significant differentiation between both samples from
375 Lofoten, and between Lofoten_2019 and Andenes (Table S4, below diagonal). In females,
376 Rockall was different from most of the other areas (i.e. Troms_Senja, Halten, Storegga_Møre,
377 North Sea, Scotland, Faroes, Iceland), but low sample size hampered the comparison with
378 Vesterålen (Table S4, above diagonal). A null overall differentiation was found among
379 individuals divided into age groups (F_{ST} = 0.000, P=0.375). While pairwise F_{ST} was significantly
380 different between the ages 4-5 years compared to age 9 or age 11, this was no longer
381 significant after the Bonferroni correction (Table S5).
382
383 After a careful evaluation of a-score patterns, 47 principal components (PCs) were retained to
384 build the DAPC plot (Figure 2). In spite of the general overlap, PC1, explaining 22.3% of the
385 variation, partially discriminated between the western and eastern Atlantic samples, whereas
386 PC2 (12.6% of the variation) did not manage to differentiate any of the remaining areas. The
387 loadings on the first axis took the highest value at 0.656 with four alleles showing values over
388 0.5 (*i.e.* NS_738_48834_T, ice_236_65321_G, NS_1604_7031_C, ice_1800_14973_A). The
389 loadings on axis 2 took the highest value at 0.702 with nine alleles exceeding 0.5
390 (Rand_394_51901_A, NS_1604_7031_A, ice_420_27575_G, NS_1596_10873_G,
391 NS_232_43461_T, ice_1800_14973_A, Rand_1772_24900_C, Rand_1076_23531_C,
392 Rand_1282_39789_A). Coordinate 1 in PCoA explained 49.62% of the variation and indicated
393 that the samples from Gulf of Maine and Rockall were different from the other areas.
394 Coordinate 2 (19.85% of the variation explained) separated first Hamarøy, and then
395 Lofoten_2019 and Røstbanken from the remaining areas (Figure 3). The F_{ST} per locus was
396 significantly different from zero at ten loci, with values ranging between 0.007 and 0.023.

The overall pattern of Isolation by Distance (IBD) was found to be driven by the furthermost geographic sample (r_{xy}=0.601, P=0.018), as significance was lost when discarding the sample from Maine (r_{xy}=0.076, P=0.247). Likewise, no pattern of isolation by distance was found among the European samples (r^2=0.006, P=0.247). No significant isolation by distance was detected for either sex (females P=0.130; males P=0.059).

3.2 Egg specific gravity measurements and temperature dependent egg stage duration

Saithe eggs began hatching as early as 6 DAF when incubated at 10°C and 13.5 DAF at 4°C. Hatching was completed within 24 h (at 6.5 DAF) at 10°C and but many eggs incubated at 4°C had still not hatched by 14 DAF. The temperature dependence of time to 50% hatching was modelled as:

$$DAF = 22.471e^{-0.141T}$$

Where DAF is days after fertilization and T is temperature in °C. The model included the data from both 2017 and 2018, with a good fit (SE= ±0.195 for the intercept and ±0.067 for slope; $r^2 = 0.95$; $p < 0.001$). The batches held at the Austevoll broodstock facility at 6.0-6.8°C reached 50% hatch at 10 DAF. Mean weighted specific density and buoyancy for North Sea saithe eggs throughout development averaged were 1.025 and 32.48 (Table 1). Saithe eggs were neutrally buoyant at a salinity of 31 – 32 during early development, increasing slightly to 33 during embryo formation, before returning to 31 close to hatching.

3.3 Individual-based model for saithe

The spatial distribution of saithe larvae for all spawning areas combined was chosen for two opposite NAO years (1990, positive NAO; 1996, negative NAO) for May 15th (Figure 4); May is

420 when the larvae should be absent from the spawning areas and arrive at the coastal nursery
421 areas. Higher low-pressure activity and stronger SW winds during the positive NAO year
422 caused a stronger northwards transport of saithe larvae. The eddy activity was considerably
423 higher in the negative NAO year, which generally translated to higher retention at the
424 corresponding spawning areas and slower northwards transport.
425
426 Connectivity matrices were used to summarize the flux of eggs and larvae between the various
427 spawning areas for 1990, a typical positive NAO year, versus 1996, a typical negative NAO year
428 (Figure 5). The retention within each box, was stronger under negative NAO years. The
429 spawning areas at Rockall (ROC) and Faroes (FAR) were particularly affected by this
430 interannual variability in wind forcing. The transport of saithe larvae along the Norwegian
431 coast was also sensitive to variable winds, with stronger transport into the northern-most box
432 (BAR) in 1990 compared to a higher residence time around Halten (middle Norway) in 1996.
433
434 The spawning area with the most stable and highest retention was Iceland, with an annual
435 mean of about 90% retained particles (Figure 6). Retention was between 50% and 60% at the
436 Rockall, Faroes, North Sea East, and Halten spawning areas, while North Sea West and Møre
437 had consistently low retention.
438
439 Most of the spawning products released at Rockall stayed either within the Rockall box or
440 were transported towards the box WOB, west of Britain (Figure 7, ref Figure 1). The
441 concentration within these two areas were negatively correlated, since all of the other areas
442 were negligible receivers and the overlap with spawning areas in the western North Sea is
443 minimal. During the years 1985-2017, less than 10% of the eggs and larvae were transported

444 towards the Faroes and the North Sea west spawning areas. The transport from Rockall to
445 WOB is strongly correlated (r=0.69) with the winter NAO index.
446

447 **4. DISCUSSION**

448 We combined genetic information on saithe population structure with individual-based
449 modeling, populated with data from laboratory-based experiments on egg specific gravity and
450 temperature-dependent development, to determine whether finer spatial population
451 structure could be defined for a species that undergoes extensive feeding and spawning
452 migrations in the North Atlantic.
453

454 Genetic differentiation, which was initially low, became non-significant assessing only the
455 Northeast Atlantic. Despite this non-result, we still find minor genetic differences in saithe
456 from Rockall compared to the surrounding areas; a finding that echoes the work by Saha et al.
457 (2015). This result was corroborated by the egg and larval transport model, which indicated
458 that local retention on the spawning grounds was generally high, averaging 62% between
459 1985 and 2017. Over this period, only 7.1% of the spawning products were transported
460 towards the western North Sea. Demographic and genetic connectivity between Rockall and
461 all other investigated spawning areas were very low.
462

463 Notwithstanding this apparent low connectivity, significant interannual variability occurs in
464 transport of eggs and larvae from Rockall to the western coast of the British Isles (WOB, Figure
465 1). Transport towards the British Isles is higher in years with strong positive NAO index. When
466 the NAO is in negative phase, the majority of spawning products are retained within the

Rockall area. Our IBM results suggest that the coastal region west of the British Isles might be an important nursery ground for Rockall saithe, a conclusion also put forward by Neat and Campbell (2011), who did not find recently settled juvenile saithe during young fish surveys at Rockall. However Saha et al. (2015) speculated that juveniles could end up in Faroes waters because only the spawning saithe, not the juveniles, were significantly different from saithe at Rockall. Because the genetic differences are persistent, adult saithe likely have some migration towards the spawning grounds in the western North Sea, but most return to the spawning grounds at Rockall.

The Northeast Arctic saithe stock are from a very large geographic area, from Møre (60° N) in the south, up to Finnmark (70° N) within the Barents Sea. Fish sampled from the Lofoten spawning grounds from 2019 were found to be genetically different from saithe around the Faroes, North Sea, and Rockall. These results support the work of Saha et al. (2015), who analyzed a single sample from much further north in the Barents Sea. These fish were also different from fish sampled in the same area in 2017. This may reflect differences due to variations in sampling locations or, more likely, mixing of spawning fish and non-spawning vagrants. Mainly immature saithe were collected in 2017 (Table S2). Surveys or fisheries do not always occur at the same time as peak spawning, which is only vaguely known for saithe (Olsen et al. 2010, Mehl et al. 2011, Homrum et al. 2012).

Sex-biased migration in saithe was though to occur because Saha et al. (2015) found significant IBD (Isolation by Distance) in female samples and Eiríksson and Árnason (2015) found a similar signal in mtDNA. We found an overall IBD pattern when comparing west and east Atlantic fish, but the pattern did not persist in females from only the northeast Atlantic. This discrepancy

might be explained by the different sampling strategies between the studies. Saha et al. (2015) included more spawning samples but from a smaller number of sites and fish than our study. The signal for sex-biased migration may not have been detected with current SNP panel, which was different from the panel in Saha et al. (2015).

The interannual variability in transport and connectivity between the spawning grounds in the North Atlantic is large. The results show higher retention at respective spawning grounds in cold years with negative NAO and increased transport northwards in warm years with positive NAO. The positive NAO years are characterized by the frequent passage of low-pressure systems resulting in a stronger northward transport of eggs and larvae, compared to years with a negative NAO index. Stronger wind forcing causes the flow to be more uniform with faster transport northwards, like in 1990. In contrast, 1996 was characterized by weaker wind forcing, causing higher eddy activity and increasing the residence time along the coast. The slower transport and retention in 1996 were also seen in the studies of movement of the Norwegian Spring Spawning herring in March and April (Tiedemann et al. 2021). During the last 30 years there has been a trend towards a more positive NAO index (Visbeck et al. 2001, Báez et al. 2021). Thus, we can speculate that the connectivity between the different spawning areas will likely be stronger in the future.

Retention within areas is generally negatively correlated with NAO, meaning that there is less retention in positive NAO years and stronger retention in negative NAO years. This signal is strongest at Rockall (r=-0.7), where there is a corresponding positive correlation between the NAO-index and transport towards the coastal region west of the British Isles. Within the North Sea, there is a negative correlation between NAO and retention at North Sea West, and a

515 corresponding positive correlation with transport into North Sea East. For particles released
516 in the North Sea East box there is a negative correlation with transport towards Møre and
517 positive with transport into the Barents Sea even though particles have to pass through Møre
518 on their path northwards. This means that the residence time within the Møre region is very
519 short, and this part of the Norwegian coast is mainly a passage more than a potential nursery
520 ground. However, interannual physical variability caused by low-pressure systems (positive
521 NAO) cause strong mixing within the North Sea (NS West to NS East) and along the Norwegian
522 coast (NS East to Barents Sea).
523
524 The dispersal connectivity also suggests a strong retention around Iceland spawning grounds.
525 However, Jakobsen and Olsen (1987) and Homrum et al. (2013) report westward migration of
526 saithe from the Norwegian coast towards the Icelandic waters. Such a basin scale migration
527 will counteract any genetic differences caused by retention of early life stages and local
528 recruitment.
529
530 The dispersal connectivity pattern supports the main biological populations proposed by the
531 genetic results, including low connectivity between Rockall and the Central Northeast Atlantic
532 genetic cluster, and high connectivity among the North Sea West and East, Faroes, Iceland and
533 the Norwegian coast. Saithe in the Northeast Atlantic appear to have less distinct population
534 structure and a high degree of connectivity, with the exception of Rockall. Low genetic
535 differentiation may be partially a result of including a large number of immature fish in the
536 analysis, where immature fish may be more likely to stray between populations. The saithe
537 management units (or stocks) are smaller than the biological population structure and may
538 therefore not inhibit sustainable harvest of this species. Mismatch between biological

539 population structure and fisheries management units can lead to overexploitation of a stock
540 (Kerr et al. 2014, Kerr et al. 2017), but this is typically when biological populations are smaller
541 than the management unit. Saithe at Rockall may be an exception; these fish are included in
542 the management of the North Sea stock, but this genetic difference indicates that it may be a
543 distinct local biological population and harvest strategies might therefore need to be revisited
544 (Kritzer & Sale 2004), as was also suggested by Saha et al. (2015).
545

546 **ACKNOWLEDGEMENTS**

547 A major motivation for the present and related studies from the Institute of Marine Research
548 (IMR) has been to resolve population structure of fish species from the commercial fisheries
549 as an aid in providing advice for management. This study was supported by the project
550 SPACEFISH in the IMR program “Biologiske prosesser”, funded by the Ministry of Trade,
551 Industry and Fisheries. Special thanks to NOAA fisheries and Professor Steven X. Cadrin
552 (SMAST) for providing the sample from Gulf of Main, to Dr.Höskuldur Björnsson (MFRI) for
553 providing the sample from Iceland. We thank Norwegian fishermen as well as crew and
554 technical staff on board our research vessels for collecting saithe samples. The egg
555 development, buoyancy and maintenance of fish, eggs and larvae at Austevoll were supported
556 by a combination of the IMR North Sea Programme and the Department of Biological Sciences
557 of the University of Bergen. We are very grateful to Alexander Beck for preparing Figure 1, to
558 Julie Skadal, Gunnar Berg, Hans Nåvik, Susanne Tonheim, Henry Seal and Endre Lygre
559 (Department of Biological Sciences, University of Bergen) for assisting with the egg
560 development and buoyancy experiments as part of the Early Life History of Fish course (BIO
561 308), and to Margareth Møgster, Annhild Engevik and Stig Ove Utskot for maintenance of the
562 saithe broodstock and the egg rearing and sampling at Austevoll. We thank the editor-in-chief

and three anonymous reviewers for constructive comments that has significantly improved the manuscript.

REFERENCES

Antao T, Lopes A, Lopes R, Beja-Pereira A, Luikart G (2008) LOSITAN: A workbench to detect molecular adaptation based on a F_{ST}-outlier method. BMC Bioinformatics 9:323

Báez JC, Gimeno L, Real R (2021) North Atlantic Oscillation and fisheries management during global climate change. Reviews in Fish Biology and Fisheries 31:319-336

Bertelsen E (1942) Contributions to the biology of the coalfish (*Gadus morhua* L.) in Faroe waters. Medd Komm Danm Fiskeri og Havunders Ser Fiskeri 11:1-69

Bjørke H, Sætre R (1994) Transport of larvae and juvenile fish into central and northern Norwegian waters. Fisheries Oceanography 3:106-119

Castaño-Primo R, Vikebø FB, Sundby S (2014) A model approach to identify the spawning grounds and describing the early life history of Northeast Arctic haddock (*Melanogrammus aeglefinus*). ICES Journal of Marine Science 71:2505-2514

Clay D, Stobo WT, Beck B, Hurley PCF (1989) Growth of juvenile pollock (*Pollachius virens* L.) along the Atlantic coast of Canada with inferences of inshore-offshore movements. J Northw Atl Fish Sci 9:37-43

Cowen RK, Lwiza KMM, Sponaugle S, Paris CB, Olson DB (2000) Connectivity of marine populations: open or closed? Science 278:857-859

Cresci A, Sandvik AD, Sævik PN, Ådlandsvik B, Olascoaga MJ, Miron P, Durif CMF, Skiftesvik AB, Browman HI, Vikebø F (2021) The lunar compass of European glass eels (*Anguilla anguilla*) increases the probability that they recruit to North Sea coasts. Fisheries Oceanography 30:315-330

Damas D (1909) Contribution à la biologie des gadides, Vol 3

Dempster T, Uglem I, Sanchez-Jerez P, Fernandez-Jover D, Bayle-Sempere J, Nilsen R, Bjørn PA (2009) Coastal salmon farms attract large and persistent aggregations of wild fish: an ecosystem effect. Marine Ecology Progress Series 385:1-14

Eiríksson GM, Árnason E (2015) Gene flow across the N-Atlantic and sex-biased dispersal inferred from mtDNA sequence variation in saithe, *Pollachius virens*. Environmental Biology of Fishes 98:67-79

EU-TOR (2020) Council Regulation (EU) 2020/123 of 27 January 2020 fixing for 2020 the fishing opportunities for certain fish stocks and groups of fish stocks, applicable in Union waters and, for Union fishing vessels, in certain non-Union waters. http://data.europa.eu/eli/reg/2020/123/oj. ST/15319/2019/INIT

Excoffier L, Laval G, Schneider S (2005) Arlequin ver. 3.0: An integrated software package for population genetics data analysis. Evol Bioinform Online 1:47-50

Fogarty MJ, Botsford LW (2007) Population connectivity and spatial management of marine fisheries. Oceanography 20:112-123

Foll M, Gaggiotti O (2006) Identifying the environmental factors that determine the genetic structure of populations. Genetics 174:875-891

Foll M, Gaggiotti O (2008) A genome-scan method to identify selected loci appropriate for both dominant and codominant markers: A Bayesian perspective. Genetics 180:977-993

Fridgeirsson E (1978) Embryonic development of five species of gadoid fishes in Icelandic waters. Rit Fiskideidar 5:1-68

Funk WC, McKay JK, Hohenlohe PA, Allendorf FW (2012) Harnessing genomics for delineating conservation units. Trends Ecol Evol 27:489-496

Gabriel S, Ziaugra L, Tabbaa D (2009) SNP genotyping using the Sequenom MassARRAY iPLEX Platform. Current Protocols in Human Genetics 60

Geffen AJ, Fox CJ, Nash RDM (2006) Temperature-dependent development rates of cod *Gadus morhua* eggs. Journal of Fish Biology 69:1060-1080

Geffen AJ, Nash RDM (2012) Egg development rates for use in egg production methods (EPMs) and beyond. Fisheries Research 117-118:48-62

Hawkins SJ, Bohn K, Sims DW, Ribeiro P, Faria J, Presa P, Pita A, Martins GM, Neto AI, Burrows MT, Genner MJ (2016) Fisheries stocks from an ecological perspective: Disentangling ecological connectivity from genetic interchange. Fisheries Research 179:333-341

Homrum Eí, Hansen B, Jónsson SÞ, Michalsen K, Burgos J, Righton D, Steingrund P, Jakobsen T, Mouritsen R, Hátún H, Armannsson H, Joensen JS (2013) Migration of saithe (*Pollachius virens*) in the Northeast Atlantic. ICES Journal of Marine Science 70:782-792

Homrum EÍ, Hansen B, Steingrund P, Hátún H (2012) Growth, maturation, diet and distribution of saithe (*Pollachius virens*) in Faroese waters (NE Atlantic). Marine Biology Research 8:246-254

Huserbråten MBO, Eriksen E, Gjøsæter H, Vikebø F (2019) Polar cod in jeopardy under the retreating Arctic sea ice. Communications Biology 2:407

Höffle H, Nash RDM, Falkenhaug T, Munk P (2013) Differences in vertical and horizontal distribution of fish larvae and zooplankton, related to hydrography. Marine Biology Research 9:629-644

ICES (2019) Advice on fishing opportunities, catch, and effort Greenland Sea and Icelandic Waters ecoregion. Saithe (*Pollachius virens*) in Division 5.a (Iceland grounds). http://ices.dk/sites/pub/Publication%20Reports/Advice/2019/2019/pok.27.5a.pdf.

ICES (2020a) ICES Advice on fishing opportunities, catch, and effort Arctic Ocean, Barents Sea, and Norwegian Sea ecoregions. Saithe (*Pollachius virens*) in subareas 1 and 2 (Northeast Arctic). http://ices.dk/sites/pub/Publication%20Reports/Advice/2020/2020/pok.27.1-2.pdf.

ICES (2020b) ICES Advice on fishing opportunities, catch, and effort Celtic Seas, Faroes, and Greater North Sea ecoregions. Saithe (*Pollachius virens*) in subareas 4 and 6, and in Division 3.a (North Sea, Rockall and West of Scotland, Skagerrak and Kattegat). http://ices.dk/sites/pub/Publication%20Reports/Advice/2020/2020/pok.27.3a46.pdf.

ICES (2020c) ICES Advice on fishing opportunities, catch, and effort Faroes ecoregion. Saithe (*Pollachius virens*) in Division 5.b (Faroes grounds). http://ices.dk/sites/pub/Publication%20Reports/Advice/2020/2020/pok.27.5b.pdf.

Jakobsen T, Olsen S (1987) Variation in rates of migration of saithe from Norwegian waters to Iceland and Faroe Islands. Fisheries Research 5:217-222

Jombart T (2008) adegenet: a R package for the multivariate analysis of genetic markers. Bioinformatics 24:1403-1405

Jombart T, Collins C (2015) A tutorial for discriminant analysis of principal components (DAPC) using adegenet 2.0.0.

651 Jombart T, Devillard S, Balloux F (2010) Discriminant analysis of principal components: a new
652 method for the analysis of genetically structured populations. BMC Genetics 11:94
653 Jung KM, Folkvord A, Kjesbu OS, Agnalt AL, Thorsen A, Sundby S (2012) Egg buoyancy
654 variability in local populations of Atlantic cod (*Gadus morhua*). Mar Biol 159:1969-1980
655 Kerr LA, Cadrin SX, Kovach AI (2014) Consequences of a mismatch between biological and
656 management units on our perception of Atlantic cod off New England. ICES Journal of
657 Marine Science 71:1366-1381
658 Kerr LA, Hintzen NT, Cadrin SX, Clausen LW, Dickey-Collas M, Goethel DR, Hatfield EMC, Kritzer
659 JP, Nash RDM, Hidalgo M (2017) Lessons learned from practical approaches to
660 reconcile mismatches between biological population structure and stock units of
661 marine fish. ICES Journal of Marine Science 74:1708-1722
662 Kritzer J, Sale P (2004) Metapopulation ecology in the sea: From Levins' model to marine
663 ecology and fisheries science. Fish and Fisheries 5:131-140
664 Lewontin RC, Krakauer J (1973) Distribution of gene frequency as a test of the theory of the
665 selective neutrality of polymorphisms. Genetics 74:175
666 Lie U (1961) On the growth and food of 0-group coal fish, *Pollachius virens* (L.), in Norwegian
667 waters. Sarsia 3:1-36
668 Lien VS, Gusdal Y, Vikebø FB (2014) Along-shelf hydrographic anomalies in the Nordic Seas
669 (1960–2011): locally generated or advective signals? Ocean Dynamics 64:1047-1059
670 Lowe WH, Allendorf FW (2010) What can genetics tell us about population connectivity? Mol
671 Ecol 19:3038-3051
672 Mehl S, Zuikova N, Drevetnyak K (2011) Saithe. In: Jakobsen T, Ozhigin VK (eds) The Barents
673 Sea - Ecosystem, Resources, Management Half a century of Russian-Norwegian
674 cooperation. Tapir Academic Press, Trondheim, Norway
675 Miller JM, Cullingham CI, Peery RM (2020) The influence of a priori grouping on inference of
676 genetic clusters: simulation study and literature review of the DAPC method. Heredity
677 125:269-280
678 Mironov NV (1961) Biology of the Barents Sea Saithe, *Pollachius virens* (L.). Int Revue ges
679 Hydrobiol 46:447-459
680 Myksvoll MS, Jung K-M, Albretsen J, Sundby S (2014) Modelling dispersal of eggs and
681 quantifying connectivity among Norwegian coastal cod subpopulations. ICES Journal
682 of Marine Science 71:957-969
683 Neat F, Campbell N (2011) Demersal fish diversity of the isolated Rockall plateau compared
684 with the adjacent west coast shelf of Scotland. Biological Journal of the Linnean Society
685 104:138-147
686 Nielsen E, Hemmer-Hansen J, Poulsen N, Loeschcke V, Moen T, Johansen T, Mittelholzer C,
687 Taranger G-L, Ogden R, Carvalho G (2009) Genomic signatures of local directional
688 selection in a high gene flow marine organism; the Atlantic cod (*Gadus morhua*). BMC
689 Evolutionary Biology 9:276
690 Nielsen EE, Cariani A, Aoidh EM, Maes GE, Milano I, Ogden R, Taylor M, Hemmer-Hansen J,
691 Babbucci M, Bargelloni L, Bekkevold D, Diopere E, Grenfell L, Helyar S, Limborg MT,
692 Martinsohn JT, McEwing R, Panitz F, Patarnello T, Tinti F, Van Houdt JKJ, Volckaert
693 FAM, Waples RS, Albin JEJ, Vieites Baptista JM, Barmintsev V, Bautista JM, Bendixen C,
694 Bergé J-P, Blohm D, Cardazzo B, Diez A, Espiñeira M, Geffen AJ, Gonzalez E, González-
695 Lavín N, Guarniero I, Jeráme M, Kochzius M, Krey G, Mouchel O, Negrisolo E, Piccinetti
696 C, Puyet A, Rastorguev S, Smith JP, Trentini M, Verrez-Bagnis V, Volkov A, Zanzi A,

Carvalho GR, FishPopTrace c (2012) Gene-associated markers provide tools for tackling illegal fishing and false eco-certification. Nature Communications 3:851

Olsen E, Aanes S, Mehl S, Holst JC, Aglen A, Gjøsæter H (2010) Cod, haddock, saithe, herring, and capelin in the Barents Sea and adjacent waters: a review of the biological value of the area. ICES Journal of Marine Science 67:87-101

Otterå H, Skilbrei OT (2014) Possible influence of salmon farming on long-term resident behaviour of wild saithe (Pollachius virens L.). ICES Journal of Marine Science 71:2484-2493

Peakall R, Smouse PE (2006) GenAlEx 6: genetic analysis in Excel. Population genetic software for teaching and research. Mol Ecol Notes 6:288-295

Pineda J, Hare JA, Sponaugle S (2007) Larval Transport and Dispersal in the Coastal Ocean and Consequences for Population Connectivity. Oceanography 20:22-39

Reiss H, Hoarau G, Dickey-Collas M, Wolff WJ (2009) Genetic population structure of marine fish: mismatch between biological and fisheries management units. Fish and Fisheries 10:361-395

Rousset F (2008) GENEPOP'007: a complete re-implementation of the genepop software for Windows and Linux. Molecular Ecology Resources 8:103-106

Russello MA, Kirk SL, Frazer KK, Askey PJ (2012) Detection of outlier loci and their utility for fisheries management. Evolutionary applications 5:39-52

Saha A, Hauser L, Kent M, Planque B, Neat F, Kirubakaran TG, Huse I, Homrum EÍ, Fevolden S-E, Lien S, Johansen T (2015) Seascape genetics of saithe (*Pollachius virens*) across the North Atlantic using single nucleotide polymorphisms. ICES Journal of Marine Science 72:2732-2741

Sandvik AD, Johnsen IA, Myksvoll MS, Sævik PN, Skogen MD (2020) Prediction of the salmon lice infestation pressure in a Norwegian fjord. ICES Journal of Marine Science 77:746-756

Sandvik H, Barrett RT, Erikstad KE, Myksvoll MS, Vikebø F, Yoccoz NG, Anker-Nilssen T, Lorentsen S-H, Reiertsen TK, Skarðhamar J, Skern-Mauritzen M, Systad GH (2016) Modelled drift patterns of fish larvae link coastal morphology to seabird colony distribution. Nature Comm 7:11599

Secor DH, Kerr LA, Cadrin SX (2009) Connectivity effects on productivity, stability, and persistence in a herring metapopulation mode. ICES J Mar Sci 66:1726-1732

Skjæraasen JE, Devine JA, Godiksen JA, Fonn M, OtterÅ H, Kjesbu OS, Norberg B, Langangen Ø, Karlsen Ø (2017) Timecourse of oocyte development in saithe *Pollachius virens*. J Fish Biol 90:109-128

Steele DH (1963) Pollock (*Pollachius virens* (L.)) in the Bay of Fundy. J Fish Res Board Can 20:1267-1314

Tiedemann M, Slotte A, Nash RDM, Stenevik EK, Kjesbu OS (2021) Drift indices confirm that rapid larval displacement is essential for recruitment success in high-latitude oceans. Front Mar Sci 8

Vikebø F, Jørgensen C, Kristiansen T, Fiksen Ø (2007) Drift, growth, and survival of larval Northeast Arctic cod with simple rules of behaviour. Mar Ecol Prog Ser 347:207-219

Vikebø FB, Korosov A, Stenevik EK, Husebø Å, Slotte A (2012) Spatio-temporal overlap of hatching in Norwegian spring-spawning herring and the spring phytoplankton bloom at available spawning substrata. ICES Journal of Marine Science 69:1298-1302

Visbeck MH, Hurrell JW, Polvani L, Cullen HM (2001) The North Atlantic Oscillation: past, present, and future. Proc Natl Acad Sci 98:12876-12877

744 Ward RD, Woodwark M, Skibinski DOF (1994) A comparison of genetic diversity levels in
745 marine, freshwater, and anadromous fishes. Journal of Fish Biology 44:213-232
746 Weir BS, Cockerham CC (1984) Estimating F-statistics for the analysis of population structure.
747 Evolution 38:1358-1370
748 Werner FE, Quinlan JA, Blanton BO, Luettich Jr. RA (1997) The role of hydrodynamics in
749 explaining variability in fish populations. Journal of Sea Research 37:195-212
750 Yaragina NA, Aglen A, Skolov KM (2011) 5.4 Cod. In: Jakobsen T, Ozhigin VK (eds) The Barents
751 Sea - Ecosystem, Resources, Management Half a century of Russian-Norwegian
752 cooperation. Tapir Academic Press, Trondheim, Norway

753

TABLES AND FIGURES

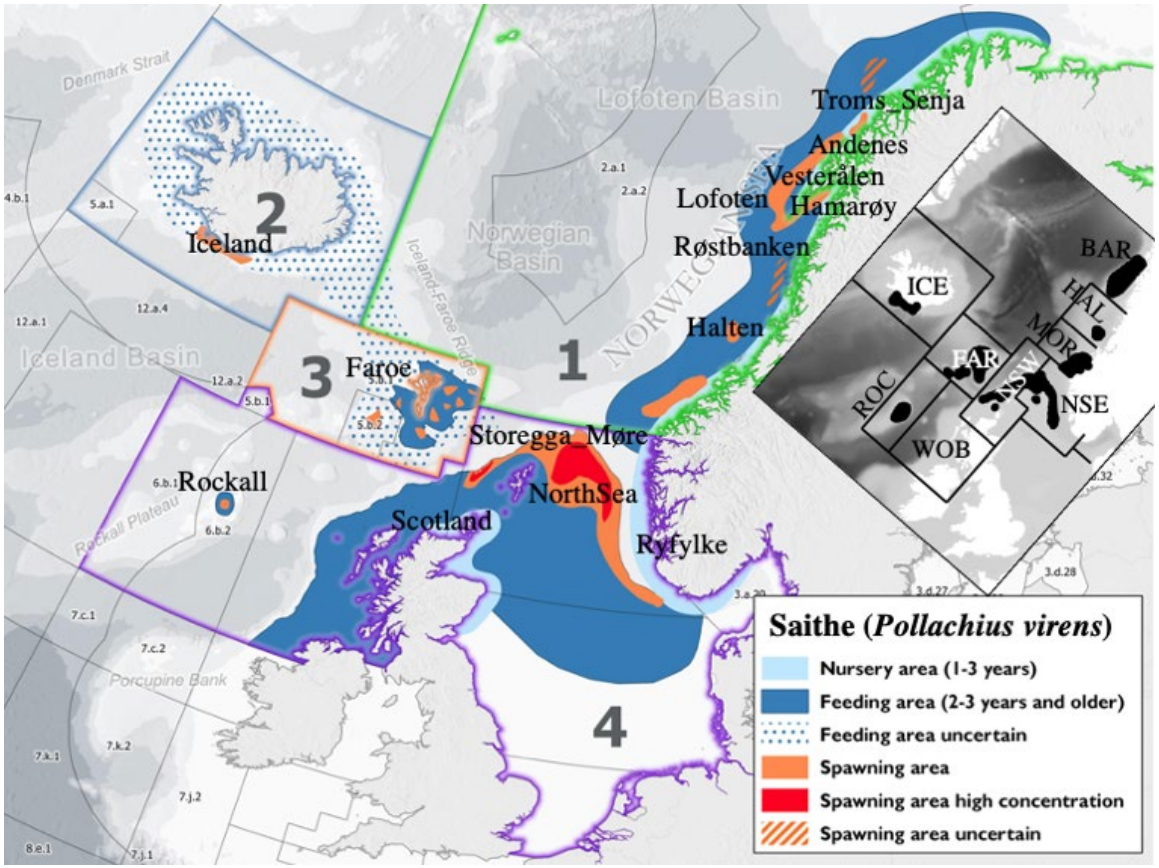

Figure 1. The distribution of saithe in the northeast Atlantic including main spawning areas, nursery areas and feeding areas, divided into four stocks as assessed by ICES; 1) Northeast Arctic, 2) Iceland, 3) Faroes, and 4) North Sea including Rockall. Geographic names refer to genetic sampling locations. The small map shows the release positions in the IBM and the zonal structure used in the connectivity analyses.

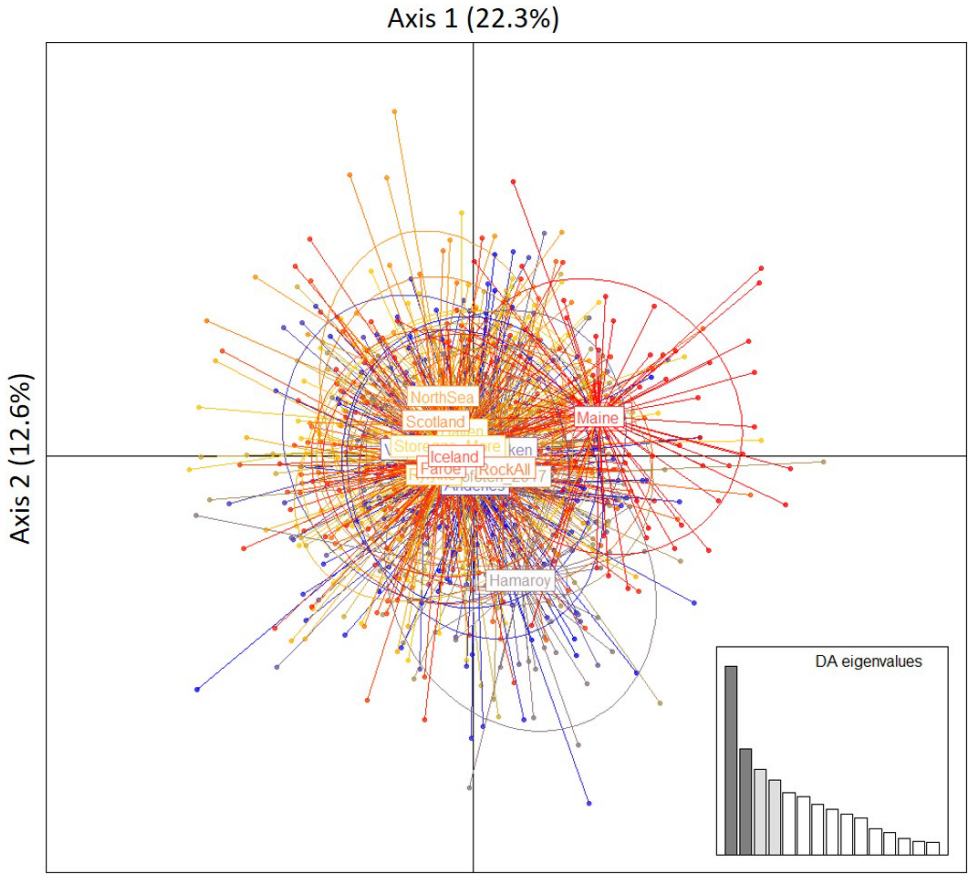

759

760 **Figure 2.** Scatterplot of the discriminant analysis of principal components (DAPC) of saithe genotyped at 64 SNP loci. Each dot represents an

761 individual, which were grouped according to geographically explicit locations

762 The horizontal axis represents the first DAPC axis (axis 1) and explains 22.3% of the variation, whereas the vertical axis represents the second

763 DAPC axis (axis 2) and accounts for 12.6% of the variation.

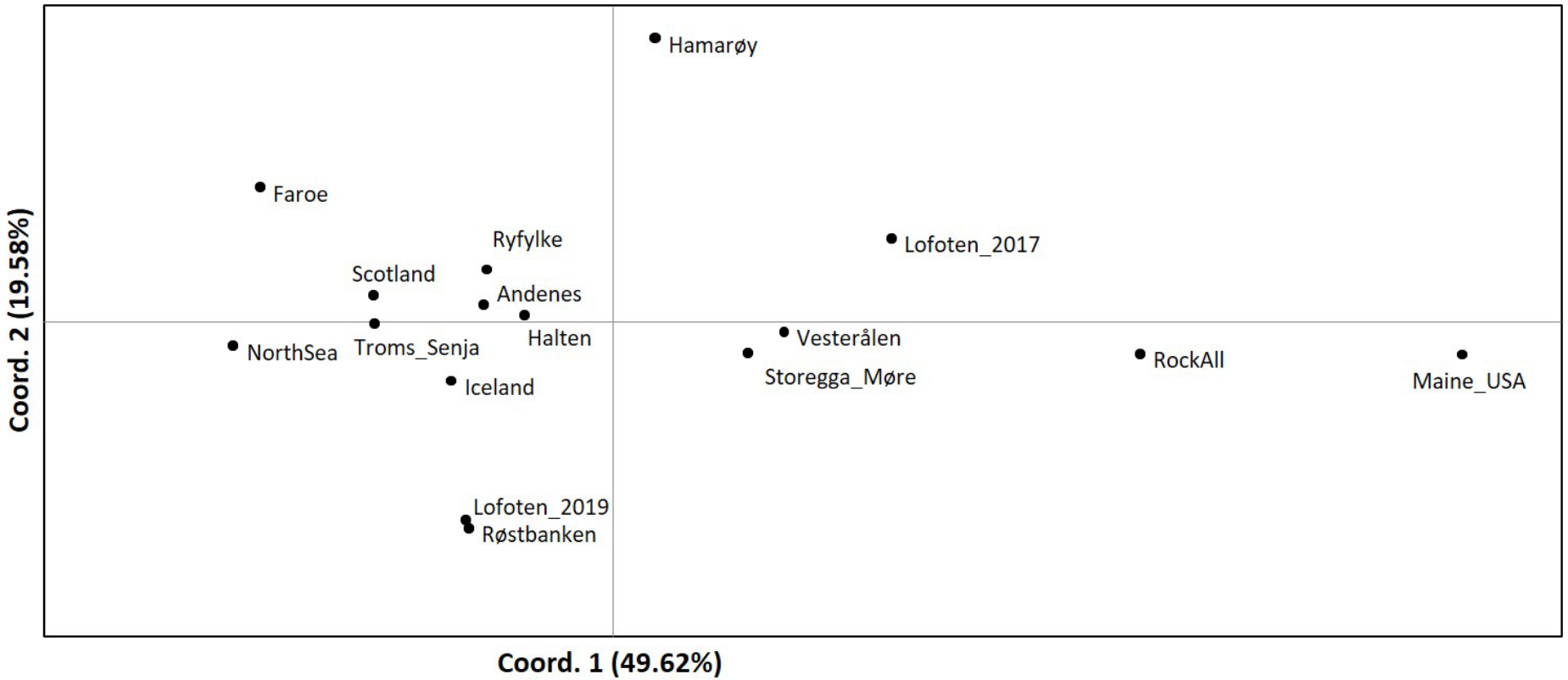

764

765 **Figure 3.** Principal Coordinates Analysis (PCoA) based on pairwise F_{ST} distances among the sixteen geographically explicit samples of saithe

766 Coordinate axis 1 accounts for 46.62 % of the variation within the data, whereas Coordinate axis 2 explains 19.58%.

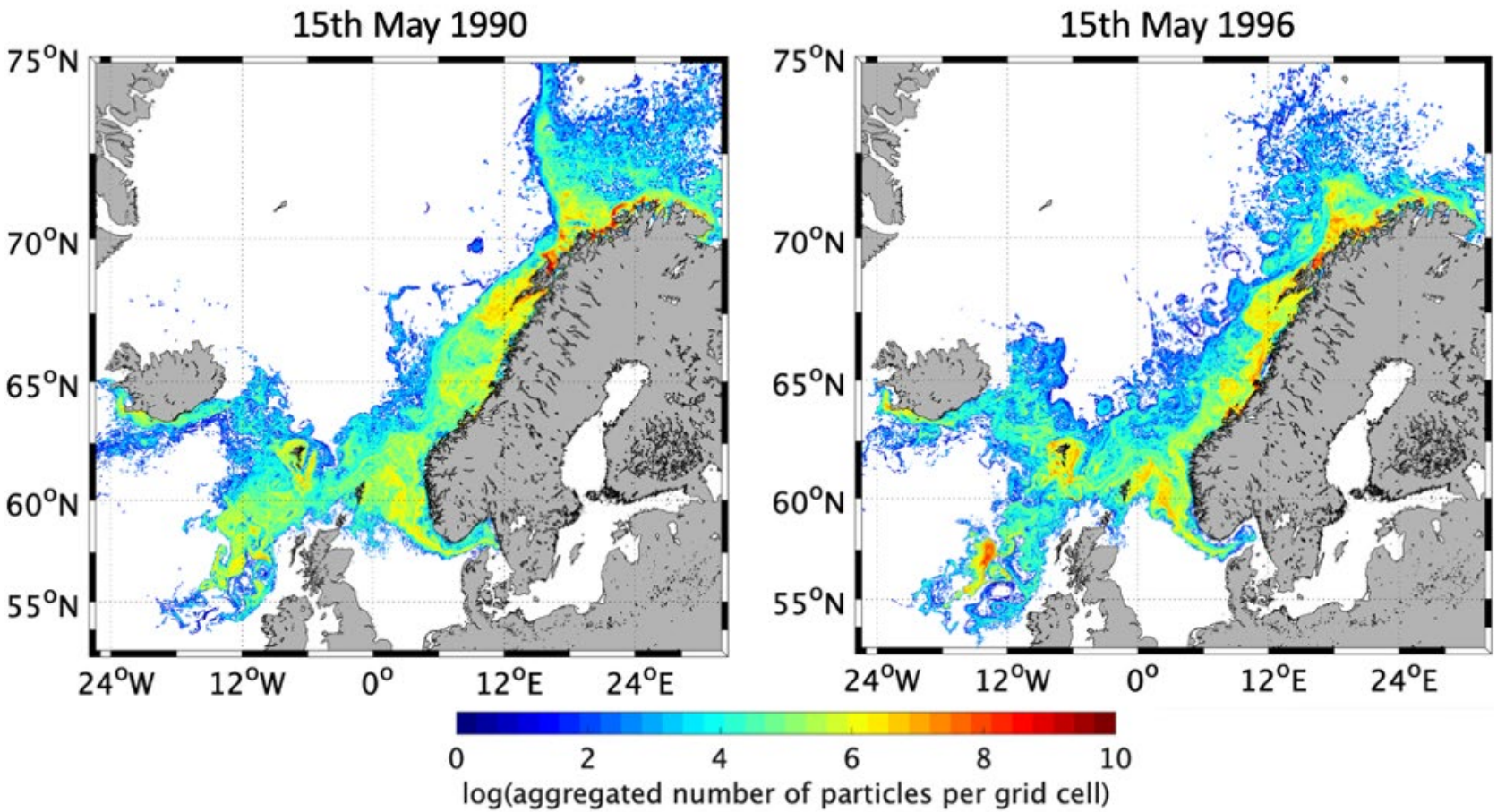

767

768 **Figure 4.** Simulated distribution of saithe eggs and larvae from all spawning areas on 15th May 1990 (left) and 15th May 1996 (right). The eggs

769 were released through February and March for all spawning areas.

770

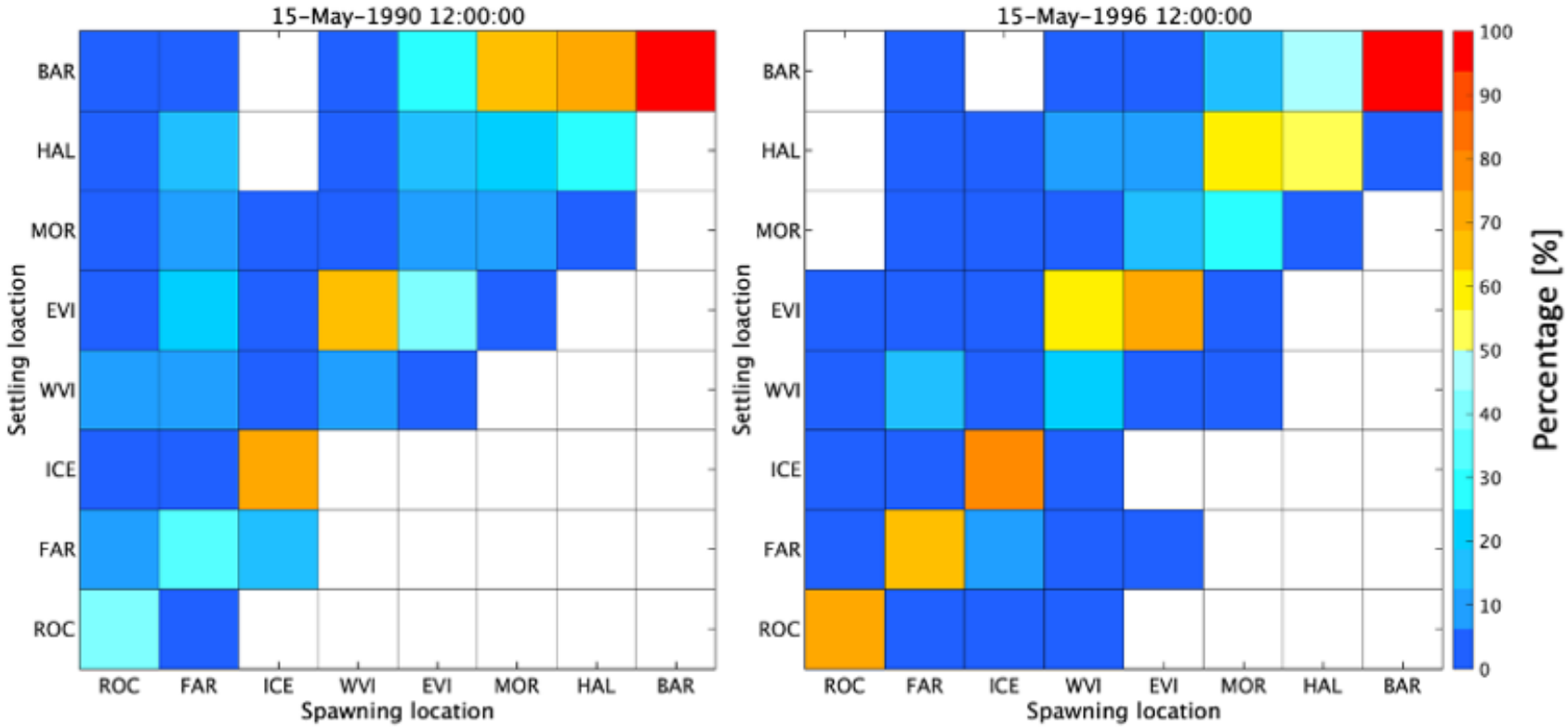

771

772 **Figure 5.** Connectivity matrices summarizing transport of particles in percentage [%] between the boxes shown in Figure S1. The x-axes specify

773 spawning location and the y-axes specify the location of the larvae on 15th May 1990 (left) and 1996 (right) after approximately three months

774 of free drift. ROC (Rockall), FAR (Faroes), ICE (Iceland), NSW (North Sea West), NSE (North Sea East), MOR (Møre), HAL (Halten), and BAR

775 (Barents Sea).

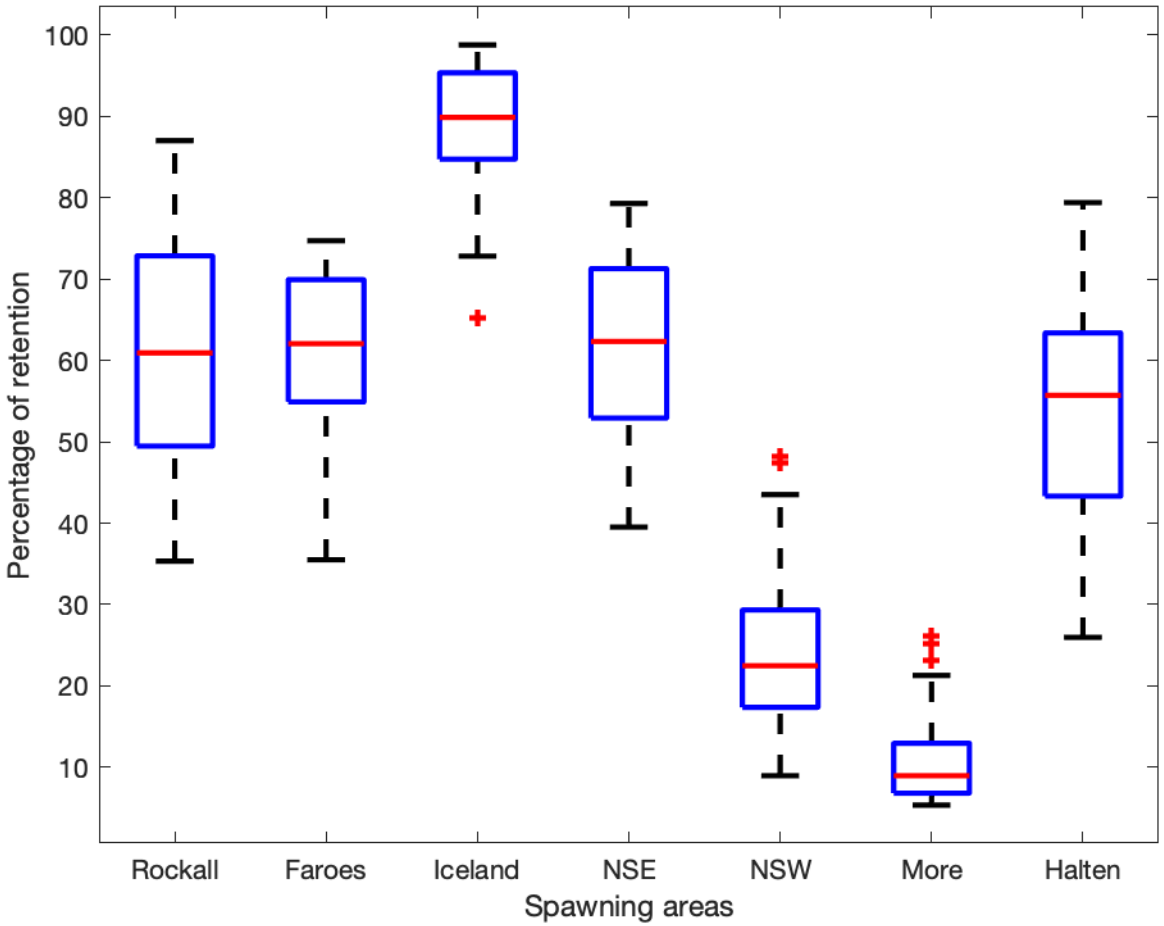
Percentage of retention
100
90
80
70
60
50
40
30
20
10
Rockall
Faroes
Iceland
NSE
NSW
More
Halten
Spawning areas

776

777 **Figure 6.** Retention for the years 1985-2017, calculated as percentage of particles that remain within the box where they were released. For
778 each box the central red mark indicates the median, the bottom and top edges of the box indicate the 25^{th} and 75^{th} percentile, the whiskers
779 extend to the most extreme data points not considered to be outliers, and the red + symbol are the outliers.
780

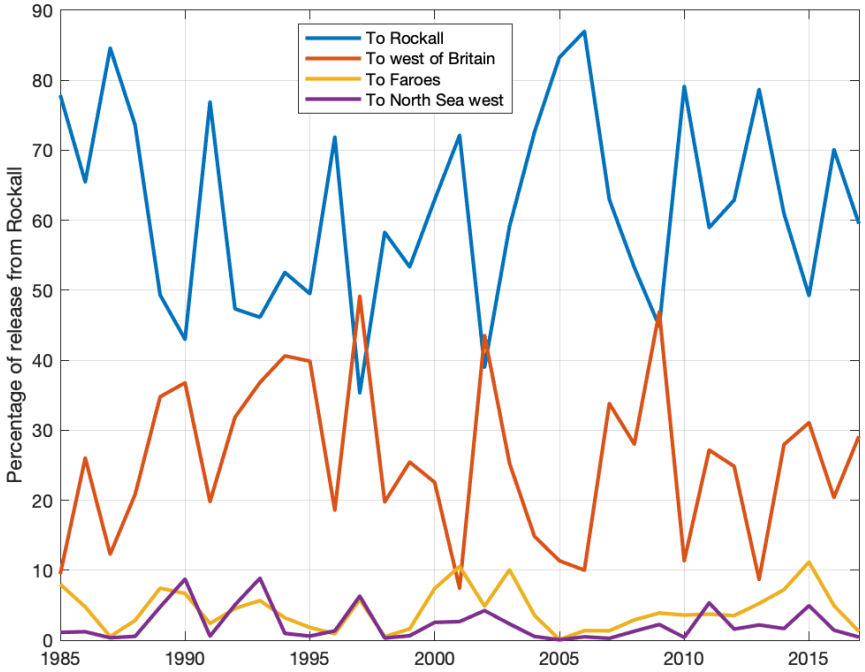

781

782 **Figure 7.** Interannual transport of eggs and larvae from the Rockall spawning area to nearby boxes, including retention (To Rockall).

783

Table 1. Mean weighted specific density and buoyancy, including standard deviation, for North Sea saithe eggs throughout development, as indicated by the stage. Temperature refers to the temperature at which the eggs were initially incubated in 2017; for 2018 eggs, it was the average temperature experienced by the eggs in the columns. Eggs in 2018 from batch 1, spawned end February, are denoted with * and batch 2, spawned mid-March with **.

Year	Temperature	Stage	Average specific density (std. deviation)		Average buoyancy (std. deviation)	
2017	4	II	1.0253	(0.0004)	32.31	(0.50)
2017	4	III	1.0257	(0.0004)	33.18	(0.53)
2017	4	III / IV	1.0257	(0.0006)	33.16	(0.73)
2017	4	V	1.0257	(0.0005)	33.15	(0.69)
2017	6	III	1.0245	(0.0002)	31.31	(0.32)
2017	6	III / IV	1.0243	(0.0007)	31.43	(0.92)
2017	6	V	1.0243	(0.0008)	31.45	(1.07)
2017	8	III	1.0252	(0.0003)	32.31	(0.44)
2017	8	IV / V	1.0247	(0.0007)	31.94	(0.93)
2018*	8	IA	1.0250	(0.0005)	32.14	(0.62)
2018*	8	IA / IB	1.0251	(0.0005)	32.43	(0.66)
2018*	8	IB	1.0257	(0.0006)	32.78	(0.73)
2018*	8	II / III	1.0258	(0.0006)	32.94	(0.78)
2018*	8	III	1.0263	(0.0009)	33.70	(1.11)
2018*	8	IV	1.0267	(0.0008)	33.93	(1.06)
2018**	8	IA	1.0242	(0.0004)	31.10	(0.45)
2018**	8	IA / IB	1.0248	(0.0006)	31.88	(0.79)
Average		All	1.025	(0.0002)	32.48	(1.14)

Table 2. Heatmap of pairwise F_{ST} (Weir & Cockerham 1984) using the suite of 64 SNPs (below diagonal) and P-values after 10000 permutations (above diagonal). F_{ST} values significantly different from zero are highlighted in boldface type and cells with borders depict significance after Bonferroni correction.

	Troms_Senja	Andenes	Vesterålen	Røstbanken	Hamarøy	Lofoten_2017	Lofoten_2019	Halten	Storegga_Møre	Ryfylke	NorthSea	Scotland	Rockall	Faroe	Iceland	Maine
Troms_Senja	*	0.4894	0.9999	0.6626	0.0945	0.4776	0.1048	0.8793	0.9893	0.6573	0.2620	0.8665	**0.0002**	0.9551	0.3239	**0.0000**
Andenes	0.0000	*	0.9999	0.1405	0.2876	0.1241	0.3284	0.2629	0.9999	0.7480	0.7416	0.8408	**0.0222**	0.3352	0.8309	**0.0000**
Vesterålen	0.0000	0.0000	*	0.9999	0.9825	0.9998	0.9999	0.9981	0.3958	0.9999	0.9484	0.9645	0.9786	0.9999	0.9999	0.3716
Røstbanken	0.0000	0.0019	0.0000	*	**0.0113**	0.1208	0.4748	0.5501	0.9999	0.2134	0.5196	0.6715	**0.0183**	0.1221	0.3945	**0.0003**
Hamarøy	0.0043	0.0012	0.0000	**0.0090**	*	0.3014	**0.0146**	0.2170	0.3003	0.4132	0.0996	0.3338	0.1486	0.3888	0.1880	**0.0046**
Lofoten_2017	0.0000	0.0021	0.0000	0.0028	0.0015	*	**0.0184**	0.4602	0.9999	0.2994	0.0551	0.5814	0.1338	0.3061	0.0576	0.5477
Lofoten_2019	0.0026	0.0005	0.0000	0.0001	**0.0086**	**0.0052**	*	0.1722	0.9578	0.8009	**0.0355**	0.5207	**0.0070**	**0.0424**	0.8666	**0.0000**
Halten	0.0000	0.0009	0.0000	0.0000	0.0020	0.0000	0.0019	*	0.5333	0.2676	0.1504	0.5964	**0.0093**	0.3816	0.5988	**0.0005**
Storegga_Møre	0.0000	0.0000	0.0004	0.0000	0.0012	0.0000	0.0000	0.0000	*	0.7453	0.9008	0.9362	0.4379	0.9584	0.9985	0.1447
Ryfylke	0.0000	0.0000	0.0000	0.0021	0.0003	0.0014	0.0000	0.0014	0.0000	*	0.1509	0.8019	**0.0305**	0.7368	0.7840	**0.0016**
NorthSea	0.0015	0.0000	0.0000	0.0000	0.0055	0.0056	**0.0057**	0.0029	0.0000	0.0039	*	0.9843	**0.0091**	0.7115	0.4039	**0.0000**
Scotland	0.0000	0.0000	0.0000	0.0000	0.0005	0.0000	0.0000	0.0000	0.0000	0.0000	0.0000	*	**0.0082**	0.9828	0.9718	**0.0008**
Rockall	**0.0108**	**0.0049**	0.0000	**0.0059**	0.0034	0.0029	**0.0068**	**0.0069**	0.0000	**0.0064**	**0.0092**	**0.0087**	*	**0.0000**	**0.0123**	**0.0206**
Faroe	0.0000	0.0005	0.0000	0.0026	0.0006	0.0011	**0.0037**	0.0004	0.0000	0.0000	0.0000	0.0000	**0.0129**	*	0.0912	**0.0000**
Iceland	0.0007	0.0000	0.0000	0.0004	0.0027	0.0029	0.0000	0.0000	0.0000	0.0000	0.0006	0.0000	**0.0056**	0.0023	*	**0.0000**
Maine	**0.0121**	**0.0102**	0.0008	**0.0105**	**0.0113**	0.0000	**0.0126**	**0.0093**	0.0023	**0.0109**	**0.0180**	**0.0123**	**0.0058**	**0.0156**	**0.0114**	*

1